



HAL
open science

Non-destructive characterization of surfaces and thin coatings using a large-bandwidth interdigital transducer

Dame Fall, Marc Duquennoy, Mohammadi Ouaftouh, Nikolay Smagin,
Bogdan Piwakowski, Frédéric Jenot

► To cite this version:

Dame Fall, Marc Duquennoy, Mohammadi Ouaftouh, Nikolay Smagin, Bogdan Piwakowski, et al.. Non-destructive characterization of surfaces and thin coatings using a large-bandwidth interdigital transducer. *Review of Scientific Instruments*, 2018, 89 (12), pp.124901. 10.1063/1.5045213. hal-03185106

HAL Id: hal-03185106

<https://hal.science/hal-03185106>

Submitted on 2 Jun 2022

HAL is a multi-disciplinary open access archive for the deposit and dissemination of scientific research documents, whether they are published or not. The documents may come from teaching and research institutions in France or abroad, or from public or private research centers.

L'archive ouverte pluridisciplinaire **HAL**, est destinée au dépôt et à la diffusion de documents scientifiques de niveau recherche, publiés ou non, émanant des établissements d'enseignement et de recherche français ou étrangers, des laboratoires publics ou privés.

Non-destructive characterization of surfaces and thin coatings using a large-bandwidth interdigital transducer

Cite as: Rev. Sci. Instrum. **89**, 124901 (2018); <https://doi.org/10.1063/1.5045213>

Submitted: 18 June 2018 • Accepted: 02 December 2018 • Published Online: 26 December 2018

Dame Fall, Marc Duquennoy,  Mohammadi Ouafitouh, et al.



View Online



Export Citation



CrossMark

ARTICLES YOU MAY BE INTERESTED IN

[Generation of broadband surface acoustic waves using a dual temporal-spatial chirp method](#)



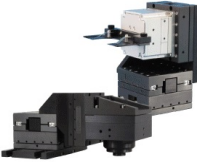
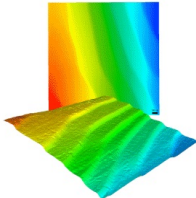
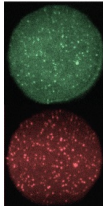
The Journal of the Acoustical Society of America **142**, EL108 (2017); <https://doi.org/10.1121/1.4994676>

[Development of interdigital transducer sensors for non-destructive characterization of thin films using high frequency Rayleigh waves](#)

Review of Scientific Instruments **82**, 064905 (2011); <https://doi.org/10.1063/1.3600797>

[DIRECT PIEZOELECTRIC COUPLING TO SURFACE ELASTIC WAVES](#)

Applied Physics Letters **7**, 314 (1965); <https://doi.org/10.1063/1.1754276>

 MCL MAD CITY LABS INC. www.madcitylabs.com	<p>Nanopositioning Systems</p> 	<p>Modular Motion Control</p> 	<p>AFM and NSOM Instruments</p> 	<p>Single Molecule Microscopes</p> 
---	--	--	---	--

Non-destructive characterization of surfaces and thin coatings using a large-bandwidth interdigital transducer

Dame Fall, Marc Duquennoy, Mohammadi Ouafitoh, Nikolay Smagin, Bogdan Piwakowski, and Frederic Jenot

Université Polytechnique Hauts de France, CNRS, Université de Lille, Yncréa, Centrale Lille, UMR 8520—IEMN, DOAE, F-59313 Valenciennes, France

(Received 18 June 2018; accepted 2 December 2018; published online 26 December 2018)

This paper deals with non-destructive testing of thin layer structures using Rayleigh-type waves over a broad frequency range (25–125 MHz). The dispersion phenomenon was used to characterize a layer-on-substrate-type sample comprising a thin layer of platinum 100 nm thick on a silicon substrate. The originality of this paper lies in the investigation of different ways of generating surface acoustic waves (SAWs) with large bandwidth interdigital transducers (IDTs) as well as the development of a measuring device to accurately estimate the SAW phase velocity. In particular, this study focuses on comparing the performance (in terms of SAW amplitude and bandwidth) of different excitations imposed on IDTs. The three types of excitations are burst, impulse, and chirp. The interest of chirp excitation compared to the other two types was clearly demonstrated in terms of the SAW bandwidth and amplitude of displacement. With these IDT transducers, measurements could be performed over a wide frequency band (20–125 MHz), and consequently, dispersion curves could be obtained over a wide frequency band with a range of velocity variations in the order of 100 m/s. Under these conditions, an extremely accurate estimate of the phase velocity as a function of the frequency could be obtained using a Slant Stack transformation. Finally, from these experimental dispersion curves and theoretical dispersion curves, an accurate estimate of the thickness of the layer could be obtained by inversion. This estimated thickness was then confirmed using profilometer measurements. *Published by AIP Publishing.* <https://doi.org/10.1063/1.5045213>

I. INTRODUCTION

Functional coatings and thin films deposited on substrates are highly sought-after in numerous applications. Such additional layers may be applied to improve the durability of structures, including wear and fatigue resistance, or to obtain specific physical or electronic properties. The characterization of these coatings and layers consists in determining their properties (thickness, elastic constants, adhesion, residual stress, etc.); it allows the state of separate structural elements to be monitored and ensures optimum operation when in use.

Among others, various ultrasonic methods have proven to be efficient for non-destructive testing (NDT) of layered structures.¹ Among the various types of ultrasonic waves that propagate near the surface boundary, Rayleigh surface acoustic waves (SAWs) are particularly interesting as their energy is concentrated within a thin layer under the surface about one wavelength thick. In the case of broadband Rayleigh wave propagation, different spectral components have non-equal penetration depths in the layer and in the substrate leading to dispersion phenomena.^{2,3}

For example, a wave with a frequency high enough to propagate entirely within the surface layer will only be affected by the characteristics of that layer. Inversely, a very low frequency wave will be mostly sensitive to the substrate characteristics. Frequency-dependent Rayleigh SAW propagation along thin coatings can be exploited to characterize the

latter.^{4–6} Indeed, given the dispersion of the SAW, it is essential in the inversion procedure used to determine the dimensional or mechanical surface characteristics to obtain a variation in the velocity of several hundreds of meters per second over the selected frequency range.⁷

Nanoscale layer thicknesses correspond to SAW wavelengths in the gigahertz frequency range. However, it has been demonstrated that even if the wavelengths are greater than a micrometer and, therefore, the thicknesses of the coatings, they remain sensitive to the characteristics of the latter.^{8–11} By generating SAW over a very high frequency range (30–300 MHz) rather than an ultra-high frequency range (300–3000 MHz), it is possible to envisage wave propagation along a coating surface of several millimeters or tens of millimeters, which is a substantial advantage in terms of characterization precision.^{4,5,12}

Several techniques have been used to generate Rayleigh-type surface waves, including laser-ultrasound,^{13–15} wedges,¹⁶ immersed transducers,¹⁷ line-focus acoustic transducers,¹⁸ or interdigital transducers (IDTs).^{4–6} The latter allows broadband SAW generation on a piezoelectric substrate in an easily controllable way using a chirped electrode finger configuration.¹⁹ Since IDTs are offset transducers for NDT applications, it is necessary to provide sustainable acoustical contact with the structure under test. This issue is sometimes circumvented by integrating IDT electrodes and the piezoelectric substrate directly into the structure^{20,21} but with unavoidable limitations regarding configurations of the samples to be characterized.

Thanks to the solution proposed (external transducer), it is possible to characterize the structures, as with conventional NDT methods, without altering or modifying the tested structures (thin layer structures).

Our original approach to resolve the issue mentioned consists in bringing a SAW-IDT, on which the fingers are deposited, in contact with the sample. In the area where the IDT piezoelectric substrate and the sample are touching, the wave is transmitted and propagates in the sample.⁴

Previously, we successfully measured the velocity dispersion on thin layer samples using a series of mono-frequency contact IDTs.⁴ In this work, we report measurements using a single wideband IDT which offers a substantial gain in measurement time and precision.²² Generally, wideband excitation signals provide lower amplitudes and a lower signal-to-noise ratio (SNR), as the signal energy is distributed over a large frequency range. However, in order to increase the SNR, it is possible to use various types of excitations for the wideband IDT. Each of these excitation approaches has its own advantages but at the expense of other measurement performances. For this reason, the purpose of the present work was to study the impact of different IDT excitation types on the results of direct dispersion measurements and on the inverse problem solution permitting to determine layer properties (thickness and elastic constants). Generally, narrowband transducers covering the desired frequency range^{4,16} or wideband transducers excited with Dirac-type pulses¹⁶ are used for SAW generation. Higher SAW amplitudes²³ can be obtained with narrowband IDTs while wideband pulsed excitation provides dense spectral data on dispersion.²² However, pulsed excitation generates lower SAW amplitudes because of the low total energy transmitted to the IDT which cannot be increased due to the limitation imposed by the piezoelectric substrate DC breakdown voltage.²⁴

We recently demonstrated that a chirped IDT could be excited with a temporal chirp (temporal-spatial chirp technique), which makes it possible to achieve higher SAW amplitudes while operating at a much lower voltage than the breakdown threshold.²⁵ In this work, we characterized a thin platinum layer (approximately 100 nm thick) deposited by thermal evaporation on a silicon (111) substrate using a chirped IDT (with 20–125 MHz frequency band) and the following three excitation types: a tone burst, a Dirac-type pulse, and a swept sine. Dispersion curves were obtained using the Slant Stack method.²⁶ The inversion procedure was then applied in order to determine the sample's characteristics. The thicknesses determined using ultrasonic measurements were compared with the profilometry data. The most appropriate excitation type for a given coating type and characterization task could then be selected from the results obtained.

The thin layer selected for this study was platinum, which is widely used in the field of microelectronics due to its very interesting mechanical and optical properties.^{27–29}

II. ESTIMATION OF PHASE VELOCITY DISPERSION

In this study, a thin layer was characterized by exploiting SAW dispersion. The measurement procedure involved

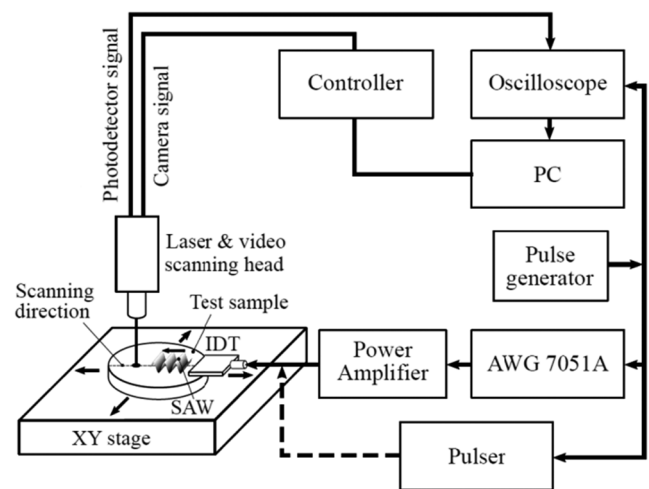


FIG. 1. Experimental setup for thin layer characterization using LDV.

several steps. First, SAWs were generated using an IDT transducer and transmitted to the test sample (Fig. 1). The waves were then detected using an interferometer sensitive to the normal displacements generated by these waves. Finally, several measurements were made at several points along the X direction in order to deduce the dispersion curves of the surface waves and, by inversion, the layer thickness. In other studies, Young's modulus and the residual stresses could be measured.^{4–6,30}

Several methods exist to determine the phase velocity dispersion from the normal displacements obtained by means of an interferometer. In our case, we chose the Slant Stack transform. This method is fast and efficient and allows the velocities to be estimated with high precision.²⁶ This method is known as τ - p transform. The signal processing makes it possible to determine the phase velocity as a function of frequency. The method is detailed, in particular, for the case of Rayleigh waves.^{31,32} In terms of precision, the results obtained with this method were as good as other methods (2DFFT, wavelet). In addition, the dispersion curves could be plotted directly.³¹

In Sec. II A, we will present the type of IDT transducer used for generating SAW and the interferometer used to measure normal displacements.

A. Interdigital transducers for generating surface acoustic waves

A SAW-IDT consists of two overlapping metal comb-shaped electrodes with interdigitated fingers and a coverage length Wa [Fig. 2(a)], where a is the finger width and b is the spacing between two consecutive fingers. The electrodes are deposited on a piezoelectric substrate. Consequently, when a voltage U is applied between the two electrodes, there is an accumulation of charges of which the signs alternate from one finger to the other thus creating an electric field between each pair of electrodes. The combination of the piezoelectric effect of the substrate and the electric field generates expansions and compressions in the material thus creating movement. It is this movement that gives rise to surface waves perpendicular to the electrode fingers. In this study, the piezoelectric plate

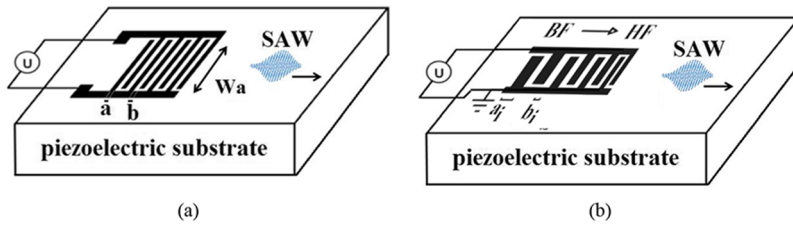


FIG. 2. Interdigital transducers for generating surface acoustic waves: (a) Narrow band IDT and (b) electrode configuration of an up-chirp IDT.

chosen was made of lithium niobate (128° YX), as this material has a very high electromechanical coupling coefficient ($K^2 = 5.3\%$).⁹

Table I presents the parameters of the chirp IDT operating between 20 and 125 MHz. In order to cover a large bandwidth with sufficiently large displacement amplitudes, particularly at high frequencies, a configuration of interdigitated chirp transducers was considered with an electrode diagram corresponding to an up-chirp configuration [Fig. 2(b)]. The number of electrodes n was equal to 149, and the period p of the electrodes was considered variable. The configuration was optimized in order to overcome high frequency attenuation of high frequency SAW.³³ The IDT active zone length was equal to 4 mm.

For the IDT excitation adapted with the dual temporal-spatial method,²⁵ a linear frequency swept signal ranging from 20 to 125 MHz with a duration of $1 \mu\text{s}$ is needed. Thus, the time-frequency product is equal to approximately 100. This is practical for applications in terms of the IDT size, total emitted energy, and Fresnel ripple level.³⁴

B. Principle of an interferometer imaging device

In order to characterize the SAW displacement field generated by this broadband IDT, we used a scanning laser Doppler vibrometer, LDV (Polytec UHF-120). This heterodyne-type apparatus allows the out-of-plane vibrational component to be measured in the frequency range from DC to 1.2 GHz. The SAW displacement sensitivity threshold is defined as $30 \text{ fm} \cdot \sqrt{f \text{ (Hz)}}$, where “fm” stands for femtometers and f is the frequency in Hertz. For $f = 125 \text{ MHz}$ and 64 averaged sweeps used in the present work, this gives a displacement noise level of approximately 30 pm. The spatial scanning resolution was defined by the motorized stages and was equal to 300 nm.

In the experimental setup (Fig. 1), the thin layer of platinum deposited on a 2-in. silicon (111) wafer was fixed on a motorized XY stage. Sensing was performed using a Polytec UHF-120 laser and video scanning head. The signal received by the scanning head’s photodiode was digitized using a LeCroy 725Zi-A oscilloscope and transferred to a personal computer (PC) for digital IQ demodulation.

The chirped and tone burst signals were generated using a Tektronix 7051 arbitrary waveform generator. Furthermore,

the signal voltage was increased to 20 V using an Amplifier Research 50W1000A power amplifier (1–1000 MHz frequency band, 50 W). For pulsed Dirac excitation, an Olympus 5900PR pulser was used instead of the arbitrary waveform generator and the power amplifier. The setup was synchronized using an external pulse generator at a rate of 20 Hz.

III. STUDY OF THE DISPERSION PHENOMENA ACCORDING TO THE CHOICE OF ELECTRICAL EXCITATION OF SAW-IDT

In this part of the paper, three types of electrical excitations are considered (burst, impulse, and chirp) to generate the SAWs with the IDTs. The influence of these three electrical excitations on the displacement amplitudes of the SAWs and on the dispersion curves is presented and illustrated in Fig. 3.

A. Burst excitation

The first type of excitation corresponds to a burst excitation. This excitation has the advantage of exciting the sensor at a determined frequency, and by choosing a sufficient number of sinusoids, it can very effectively excite the transducer and consequently produce significant SAW amplitudes. In order to test the performance of the transducers over their entire bandwidth, several bursts were tested at 30, 50, 70, 90, and 110 MHz. For each of the frequencies, measurements were conducted using an interferometer at $N = 41$ points at intervals of $\Delta x = 500 \mu\text{m}$. The amplitude of electrical excitation was 20 V as the chirp excitation [Fig. 3(c), top]. For example, a SAW displacement waveform for 10 cycles of a 70 MHz burst exhibits a 1.4 nm amplitude. Thus, thanks to the good signal-to-noise ratio (the noise was almost invisible), it was possible to reduce the number of measurement points N (41 with this excitation) because with the Slant stack method, the number of points N also depends on the signal-to-noise ratio. In Fig. 4, the set of spectra (in red) and their average (in black) are plotted. The dispersion curve is plotted in Fig. 5. However, for measurements over large frequency bands, several frequencies must be used in order to cover the selected frequency range. For each frequency chosen, a new LDV scan is necessary.

It is possible to observe the dispersion phenomenon which extends from approximately 4525 to 4450 m/s (Fig. 5). Given that each burst is composed of 10 sinusoids, it can also be seen that the results of the inversions are valid over a certain bandwidth increasing gradually from 5.14 MHz for an excitation at 30 MHz to 16.8 MHz for an excitation at 110 MHz (Fig. 4).³⁷ Compared with the solution proposed in the article of Deboucq *et al.*⁴ where single-frequency

TABLE I. Parameters of up-chirp IDT.

fo (MHz)	n	Wa (mm)	a (μm)	b (μm)	P (μm)	λ (μm)
(20-125)	149	2, 5	(8-50)	(8-50)	(16-100)	(32-200)

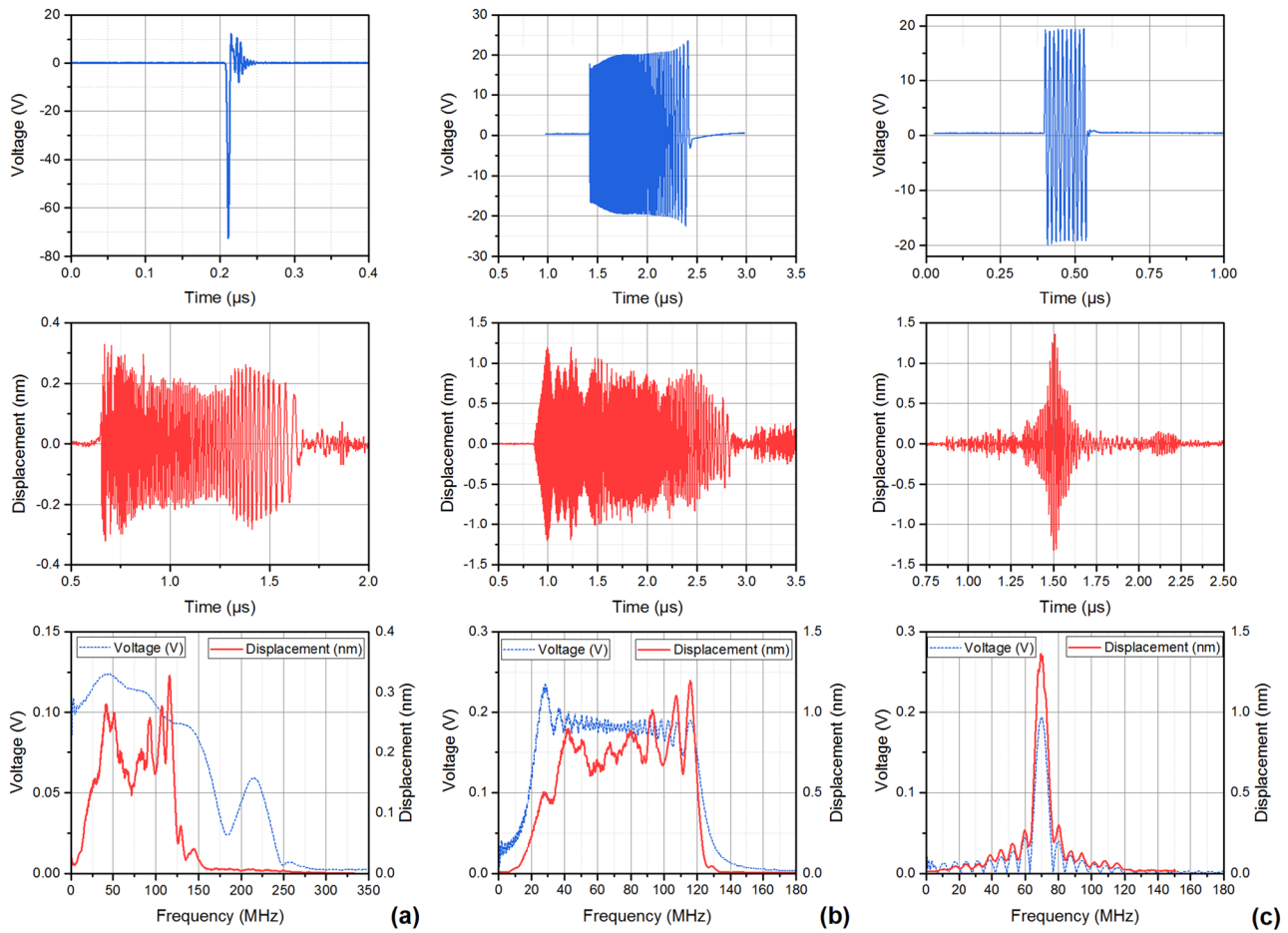


FIG. 3. From top to bottom: electrical signal, SAW displacement, and corresponding frequency spectra for impulse (a), chirp (b), and burst (c) excitations of the IDT.

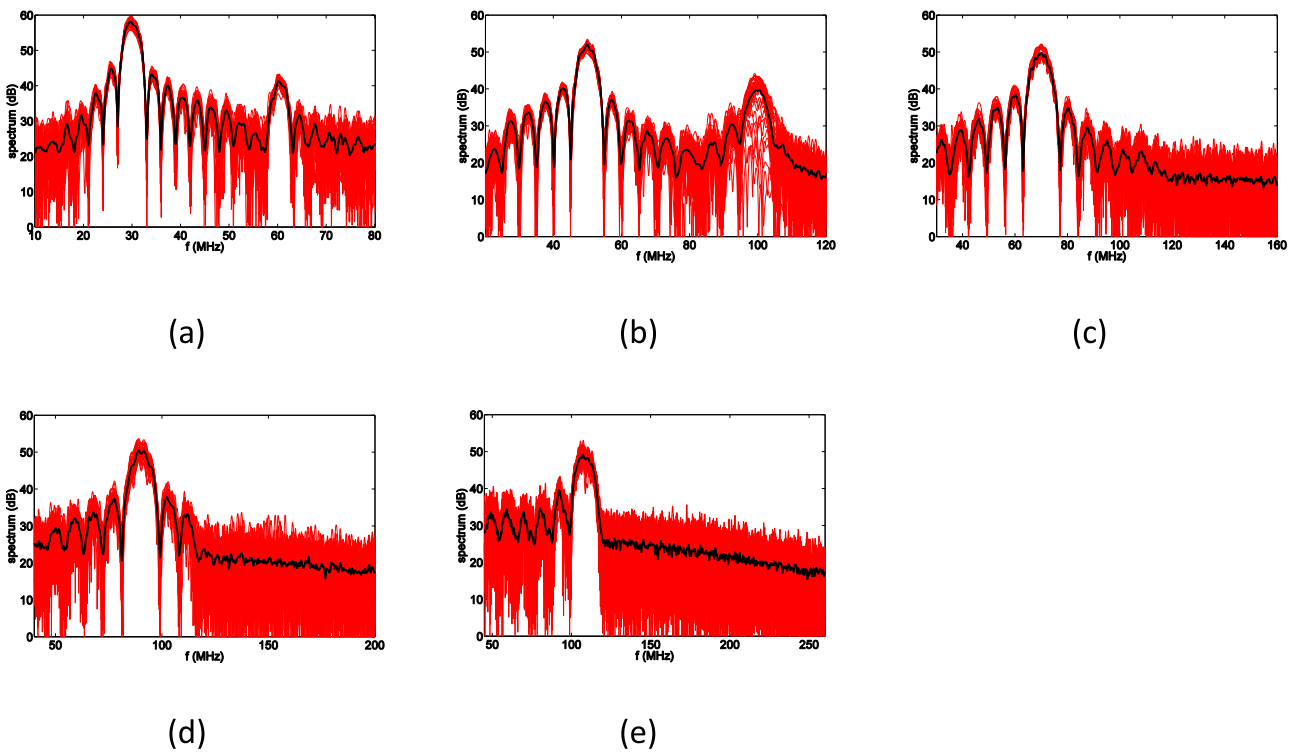


FIG. 4. All the spectra (in red) and their average (in black) displacement for a burst excitation: (a) 30 MHz, (b) 50 MHz, (c) 70 MHz, (d) 90 MHz, and (e) 110 MHz.

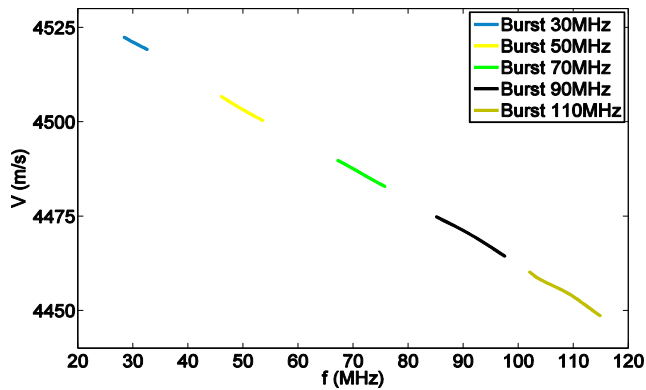


FIG. 5. Dispersion curves obtained for the 5 burst excitations.

transducers were favored, not only the total bandwidth was increased (25–115 MHz instead of 5–45 MHz) but also a single broadband IDT could perform all the measurements instead of 8 previously. This solution avoids multiplying the number of IDTs to obtain a dispersion curve over a wide frequency range, but also reduces the number of handling steps to ensure IDT/sample contact.

B. Impulse excitation

The second type of excitation corresponds to an impulse excitation (Dirac-type pulse).

The main advantage of Dirac-type pulse excitation is its suitability for any type of narrow or wideband transducers provided that the pulse frequency band covers that of the transducer. Pulsed excitation directly reveals the impulse response of the transducer. However, this signal provides a low signal-to-noise ratio due to the low total spectrum energy emitted but over a very short time interval.

This Dirac-type pulse was imposed on the transducer making it possible to determine the spectral content of the transducer transfer function directly. However, due to the small distances between the electrodes determined by the frequency (minimum 8 μm) and the dielectric strength of lithium niobate,^{35,36} it was necessary to limit the amplitude of the Dirac pulses to a peak voltage of 100 V, which limits the amplitude of the SAW.²⁴

The waveform of such signals generated with an Olympus 5900PR pulser at 1 μJ is shown in Fig. 3(a), top. The signal bandwidth is approximately 150 MHz [blue

dotted-dashed curve, bottom, Fig. 3(a)]. The amplitude envelope of the corresponding SAW displacement waveform measured directly on the LiNbO₃ substrate close to the IDT aperture was approximately 200 pm [Fig. 3(a), middle]. All the frequency spectrum components between 20 and 125 MHz were present in the signal generated [Fig. 3(a), bottom].

Measurements were conducted using an interferometer at $N = 201$ points at intervals of $\Delta x = 100 \mu\text{m}$. The SAW displacement waveform of 0.2 nm corresponds to a decrease of 85% compared to the amplitude of the same frequency component of the burst signal [Fig. 3(a), middle].

In Fig. 6(a), all the spectra (in red) and their average (in black) are plotted. The dispersion curve obtained with the Slant stack method is plotted in Fig. 6(b). From this spectrum [Fig. 6(a)], it is possible to observe that the transducer covers the entire frequency band between 20 and 125 MHz. In Fig. 6(b), the dispersion curve over the entire transducer bandwidth is presented. The dispersion phenomenon ranged from approximately 4525–4425 m/s.

C. Chirp excitation

The third type of excitation envisaged was a chirp excitation. This excitation has the advantage of exciting the SAW over the entire bandwidth and provides higher displacement amplitudes than those obtained with an impulse excitation.²⁵ Indeed, this type of excitation allows the transmission of a significant amount of energy that is distributed over time. This makes it possible to impose an input voltage on the well-adapted transducer and thus to avoid breakdown phenomena.

The chirp excitation amplitude was $20 V_{\text{peak}}$, which was more than 5 times lower than the pulse excitation amplitude. The duration of the chirp excitation was 1 μs , and it was calculated taking into account the length of the IDT ($L = 4 \text{ mm}$) and the velocity of propagation of the SAW ($c = 4000 \text{ m/s}$). Again, the measurements were conducted using an interferometer at $N = 201$ points at intervals of $\Delta x = 100 \mu\text{m}$.

The electrical signal of this chirp excitation for a 50 Ω load impedance is presented in Fig. 3(b), top. The average amplitude envelope of 20 V was selected to obtain a sufficient SAW displacement possible while operating the IDT under safe conditions.

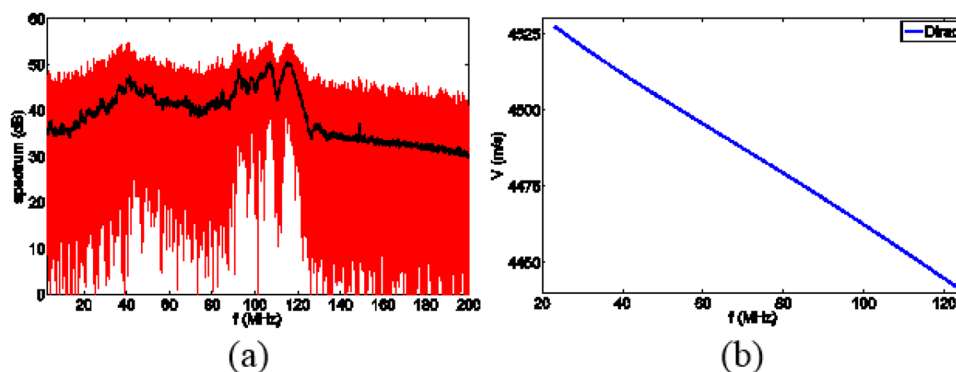


FIG. 6. (a) All the spectra (in red) and their average (in black) displacement for an impulse excitation and (b) dispersion curve obtained with an impulse excitation.

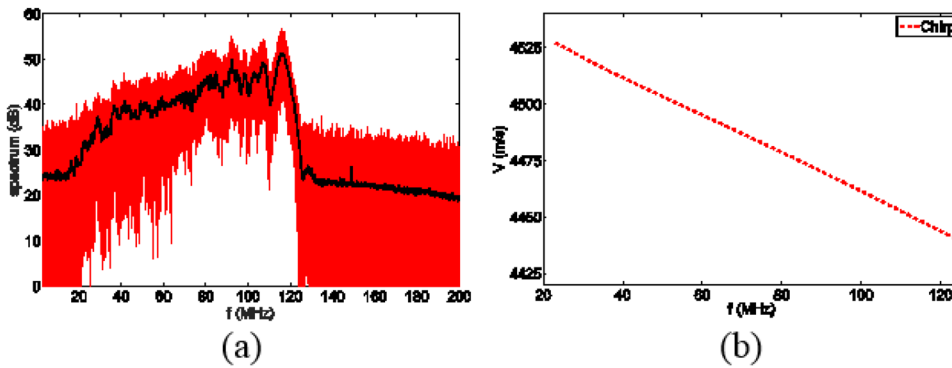


FIG. 7. (a) All the spectra (in red) and their average (in black) displacement for a chirp excitation and (b) dispersion curve obtained with a chirp excitation.

The non-rectangular shape of the waveform envelope seen in Fig. 3(b) is due to the amplifier's frequency band imperfections. The corresponding SAW displacement waveform measured using LDV exhibits an average envelope amplitude of approximately 800 pm, which is 4 times greater than that with a pulsed excitation. The difference in excitation and response signal spectra is due to the particularities of the IDT transfer function optimized for high frequency emissions.³³

In Fig. 7(a), all the spectra (in red) and their average (in black) are plotted. The dispersion curve is plotted in Fig. 7(b). As with an impulse excitation, it can be observed that the transducer covers the entire frequency band between 20 and 125 MHz [Fig. 7(a)]. In Fig. 7(b), the dispersion curve, extending from 4525 to 4425 m/s as with a pulse excitation, is presented over the entire transducer passband.

D. Comparison of the SAW displacement amplitude for the impulse and chirp excitations on a platinum layer on a silica substrate

As shown previously, chirp excitation offers the same capacity as impulse excitation to excite SAWs over the entire bandwidth, with the additional possibility of multiplying the SAW displacement amplitude by 4 in relation to an impulse excitation.

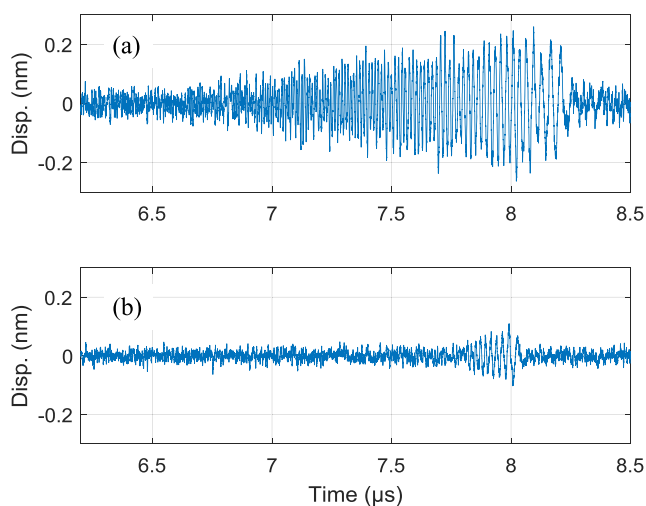


FIG. 8. SAW displacement for chirp (a) and impulse (b) excitations of the IDT on a silica substrate.

To illustrate this, and since the platinum/silicon sample is relatively non-attenuating, we present the echograms and the associated spectra obtained on a silica sample (more attenuating) covered with a silica sol-gel layer (Fig. 8). To achieve these figures, the transducer was positioned at a distance of 20 mm from the detection point. Figure 9 presents the surface displacement where the SAW passes through. It is very clear that for the impulse excitation only the low frequency components are not completely attenuated. Conversely, all the components remain in the signal for the chirp excitation. This illustrates and proves the interest of chirp excitation compared to impulse excitation.

E. Comparison of the dispersion curves for the three types of excitations on a platinum layer on a silicon substrate

Figure 10 shows all the **dispersion curves** obtained with the three types of excitations. This representation makes it possible to verify that all the excitations used led to similar results. By superimposing the previous results obtained with the burst excitation and those obtained with the impulse and chirp excitations, a perfect overlap can be observed (Fig. 10).

In this case (platinum/silicon sample), the attenuation is not very strong and the displacement amplitudes obtained with the 3 types of excitations are maximum amplitudes equal to 200 pm, 800 pm, and 1400 pm for the impulse, chirp, and burst excitations, respectively. Since the Slant Stack transformation

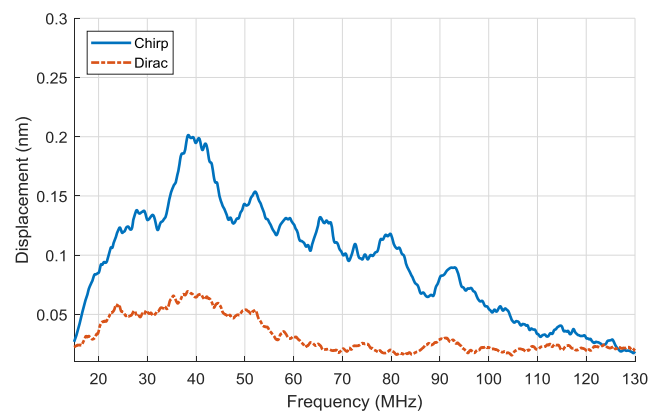


FIG. 9. Frequency spectra corresponding to the displacement for impulse and chirp excitations of the IDT on a silica substrate.

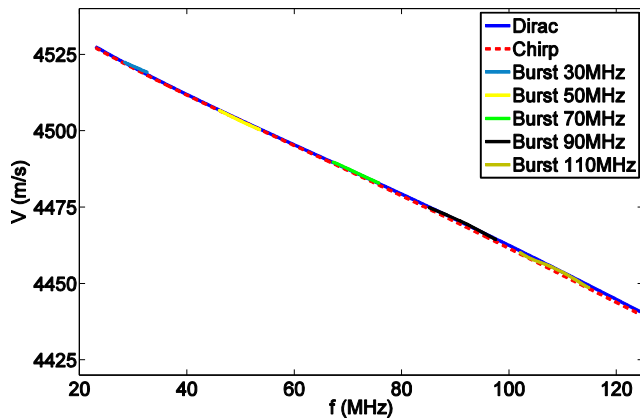


FIG. 10. Dispersion curves obtained for all the excitations.

is a robust method, the dispersion curves obtained for each of the excitations are in very good agreement.

IV. INVERSE PROBLEMS AND EXPERIMENTAL CHARACTERIZATION OF THE LAYER-ON-SUBSTRATE STRUCTURE

Since the dispersion curves are directly related to the elastic properties and the densities of the two materials, as well as to the thickness of the layer, they can be calculated theoretically.³⁸ In our case, the densities of the platinum layer and the silicon substrate were known accurately^{39,40} and the estimation of the layer thickness from the phase velocities measured consisted in solving the inverse problem. An inverse method was used to determine the thickness, which provides theoretical propagation velocities that are as close as possible to those measured experimentally. The optimization method selected thus allows theoretical velocities that are the closest to the measured velocities to be obtained.

The approximate values of the elastic coefficients from the bibliographic data^{39,40} provided an initial estimate of the phase velocities (Table II). A minimization routine was then executed to find the thickness of the layer. A least squares minimization was carried out. The processing algorithm then sought to maximize the value of the coefficient of determination.⁴

For the inverse method procedure, we defined thicknesses between 80 and 130 nm with a step of 0.002 nm. The dispersion curve was plotted using different thickness values (Fig. 11). Finally, the estimated layer thickness was 118 nm.

TABLE II. Characteristics of the platinum layer are considered as isotropic; the orientation of the silicon wafer is 111, and direction of wave propagation is 110.

	Platine layer	Silicium wafer
Density ρ (g/cm ³)	21.45	2.33
Longitudinal wave velocity (m/s)	3976.1	8726
Shear wave velocity (m/s)	1688.5	4969.4
Rayleigh wave velocity (m/s)	1593.6	4548

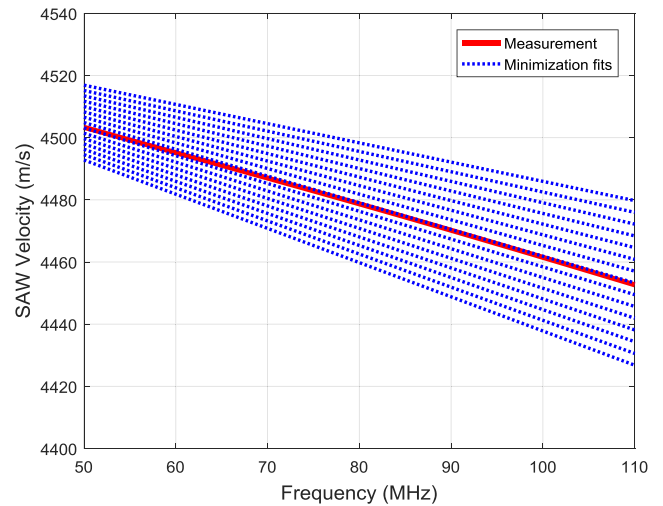


FIG. 11. Theoretical and experimental dispersion curves.

The thicknesses determined using our inversion procedure were compared with the measurements obtained using a KLA-Tencor Asic surface profiler. The uncertainty of the thickness estimation was about ± 5 nm. Several non-covered regions were intentionally left near the boundaries of the sample. The “steps” formed between the platinum-covered and non-covered regions permitted profilometer measurements. In numerous practical cases, such measurements are not possible due to the absence of such features.

The measurements yielded average layer thicknesses of 114 nm, that is to say, small differences of 3.4%. It is important to note that these profilometer measurements are highly accurate locally (step height) but do not allow accurate estimates outside the steps, that is to say, over “long distances” and, in particular, for samples several tens of millimeters long.

V. DISCUSSION

The results presented above clearly highlight the great interest of a chirp wideband IDT for NDT of thin layers. Using a wideband Rayleigh source with a 20–125 MHz frequency range, a variation in SAW velocity in the order of 100 m/s can be obtained for layers of thickness varying from some tens to several hundreds of nanometers. Thus, using only a single IDT and a single LDV longitudinal scanning, it is possible to measure an entire dispersion curve. This results in a substantial gain in measurement time compared with covering the required frequency band with sets of single-frequency IDTs.⁴

However, if a SAW displacement amplitude generated by a single electrode pair is the same for chirped and mono-frequency IDT configurations, when using IDTs with many finger pairs, the resulting displacement amplitude of a SAW envelope will be higher for the latter IDT configuration. This is due to the fact that the constructive SAW interference cannot be completely exploited in the chirped configuration.⁹

One of the objectives of this work was to investigate if the lower SAW displacement amplitude provided by wideband IDT would be sufficient for dispersion measurements

using the Slant Stack method. First, we used a common Dirac-type pulse excitation with a 70 V amplitude (below the 100 V limit) and a bandwidth of approximately 150 MHz. The platinum-coated sample studied exhibits low SAW attenuation. As a result, this excitation provided SAW displacement amplitudes of approximately 200 pm and a SNR of 20 dB. Even with a rather low SNR, accurate measurement of the velocity dispersion is possible.

However, for highly attenuating samples such as PDMS,^{6,30} 200 pm SAW displacements may not be sufficient for propagation over several centimeters and the SNR issue could become vital. For this reason, we studied an adapted chirped excitation in the same 20–125 MHz frequency range. As a result, the SNR was improved by up to 32 dB (correspondingly to an average SAW amplitude of 800 pm) over the whole frequency range. The calculated velocity dispersion corresponding to the Dirac-type and chirped excitations were almost identical and exhibited a discrepancy of 0.02%.

Furthermore, an increase in the SNR was possible by applying a quasi-narrowband tone burst excitation on a wideband IDT. The SAW displacement amplitude was increased by 75% (up to 1.4 nm), and the corresponding SNR value was 37 dB. However, in order to cover a variation in the velocity of 100 m/s, measurements over a broad bandwidth requiring 5 different sensors were necessary.

It is worth mentioning that narrowband excitation of a wideband IDT does not allow the same SAW displacements to be achieved compared with single mono-frequency IDTs. As an example, we performed measurements with a 30 MHz IDT consisting of 10 finger pairs. This IDT was made of the same materials, and the same photolithography process as the chirped one was used.

For the 10 identical tone burst excitation cycles, as reported for the previous series of measurements, the SAW displacement amplitude generated with the mono-frequency transducer reached 3.2 nm, which corresponds to a 44 dB SNR. However, an approach like this requires acoustical contact to be established for each of the IDTs, which is rather time-consuming.

VI. CONCLUSION

We used a wideband chirp IDT for the non-destructive characterization of thin layers deposited on a silicon substrate and compared three types of time excitations: burst, impulse, and chirp. The results obtained clearly show the great interest of using the latter. Indeed, it offers the advantage of a burst excitation, in other words, a sufficiently high SAW displacement amplitude and the advantage of an impulse excitation, i.e., a wide frequency band for measurement.

Experimental dispersion curves were obtained using the Slant Stack transformation, and we can conclude that this one is a robust method for the characterization of thin layers and is compatible with any type of excitation of a wideband SAW-IDT. The sample thickness was determined by solving the inversion problem, and a 3.4% difference was obtained compared with the profilometry data.

In applications using IDTs for the non-destructive testing or characterization of thin layer materials, these sensors are often integrated in the structures to be tested. This imposes additional constraints when creating special test samples (metal deposit, for example, on the surface to be controlled). In this work, the IDT was not integrated in the structure. We chose basic contact between the IDT and the sample using a coupling medium, which obviously offers the possibility of using the IDT with the same facilities as conventional sensors. Finally, proposing remote sensors also makes it possible to prevent damage to the structures being tested (even fragile), and there are no preparation steps.

ACKNOWLEDGMENTS

The ELSAT2020 project was co-financed by the European Union through the European Regional Development Fund, the French government, and the Hauts de France Regional Council. This work was also supported by the French RENATECH network.

- ¹D. O. Thompson and D. E. Chimenti, *Review of Progress in Quantitative Nondestructive Evaluation* (Springer, USA, 2012).
- ²K. Sezawa, *Bull. Earthquake Res. Inst., Univ. Tokyo* **3**, 1 (1927).
- ³N. A. Haskell, *Bull. Seismol. Soc. Am.* **43**, 17 (1953).
- ⁴J. Deboucq, M. Duquennoy, M. Ouaftouh, F. Jenot, J. Carlier, and M. Ourak, *Rev. Sci. Instrum.* **82**, 064905 (2011).
- ⁵M. Duquennoy, M. Ouaftouh, J. Deboucq, J.-E. Lefebvre, F. Jenot, and M. Ourak, *Appl. Phys. Lett.* **101**, 234104 (2012).
- ⁶D. Fall, F. Compoin, M. Duquennoy, H. Piombini, M. Ouaftouh, F. Jenot, B. Piwakowski, P. Belleville, and C. Ambard, *Ultrasonics* **68**, 102 (2016).
- ⁷J. J. Ditre and D. Hongerholt, *Int. J. Solids Struct.* **33**, 2437 (1996).
- ⁸C. Campbell, *Surface Acoustic Wave Devices for Mobile and Wireless Communications*, 1st ed. (Academic Press, Inc., Orlando, FL, USA, 1998).
- ⁹D. Royer and E. Dieulesaint, *Elastic Waves in Solids* (Springer, Berlin, 2000).
- ¹⁰C. Campbell, *Surface Acoustic Wave Devices for Mobile and Wireless Communications* (Academic Press, San Diego, 1998).
- ¹¹D. Royer and E. Dieulesaint, *Elastic Waves in Solids II: Generation, Acousto-Optic Interaction, Applications* (Springer Science & Business Media, 1999).
- ¹²M. Duquennoy, M. Ouaftouh, J. Deboucq, J.-E. Lefebvre, F. Jenot, and M. Ourak, *J. Acoust. Soc. Am.* **134**, 4360 (2013).
- ¹³A. Lomonosov, A. P. Mayer, and P. Hess, *Handbook of Elastic Properties of Solids, Liquids, and Gases* (Academic Press, New York, 2001), pp. 137–185.
- ¹⁴A. Ruiz and P. B. Nagy, *Instrum. Meas. Metrol.* **3**, 59 (2003).
- ¹⁵J. Goossens, P. Leclaire, X. Xu, C. Glorieux, L. Martinez, A. Sola, C. Sili-gardi, V. Cannillo, T. Van der Donck, and J.-P. Celis, *J. Appl. Phys.* **102**, 053508 (2007).
- ¹⁶B. R. Tittmann, L. A. Ahlberg, J. M. Richardson, and R. B. Thompson, *IEEE Trans. Sonics Ultrason., Ferroelectr. Freq. Control* **34**, 500 (1987).
- ¹⁷F. Lakestani, J.-F. Coste, and R. Denis, *NDT & E Int.* **28**, 171 (1995).
- ¹⁸P. D. Warren, C. Pecorari, O. V. Kolosov, S. G. Roberts, and G. A. D. Briggs, *Nanotechnology* **7**, 295 (1996).
- ¹⁹R. H. Tancrell and M. G. Holland, *Proc. IEEE* **59**, 393 (1971).
- ²⁰K. Toda, G. Sugizaki, T. Takenaka, and K. Sakata, *Sens. Actuators A-Phys.* **43**, 213 (1994).
- ²¹T.-T. Wu, Y.-Y. Chen, G.-T. Huang, and P.-Z. Chang, *J. Appl. Phys.* **97**, 073510 (2005).
- ²²J. M. Richardson, *J. Appl. Phys.* **48**, 498 (1977).
- ²³D. P. Morgan, *Surface-Wave Devices for Signal Processing* (Elsevier, Amsterdam, The Netherlands, 1991), pp. 129–151.
- ²⁴F. S. Hickernell, P. L. Clar, and I. R. Cook, in *1972 Ultrasonic Symposium* (IEEE, 1972), pp. 388–391.
- ²⁵D. Fall, M. Duquennoy, M. Ouaftouh, N. Smagin, B. Piwakowski, and F. Jenot, *J. Acoust. Soc. Am.* **142**, EL108 (2017).

- ²⁶G. McMechan and M. Yedlin, *Geophysics* **46**, 869 (1981).
- ²⁷N. M. Davey and R. J. Seymour, *Platinum Met. Rev.* **29**, 2 (1985).
- ²⁸P. D. Gurney and R. J. Seymour, in *Studies in Inorganic Chemistry*, edited by F. R. Hartley (Elsevier, 1991), pp. 594–620.
- ²⁹A. Seignac and M. S. Robin, *Solid State Commun.* **11**, 217 (1972).
- ³⁰F. Compoint, D. Fall, H. Piombini, P. Belleville, Y. Montouillout, M. Duquennoy, M. Ouaftouh, F. Jenot, B. Piwakowski, and C. Sanchez, *J. Mater. Sci.* **51**, 5031 (2016).
- ³¹L. Ambrozinski, B. Piwakowski, T. Stepinski, and T. Uhl, *NDT & E Int.* **68**, 88 (2014).
- ³²R. Askari and S. Hejazi, *Geophysics* **80**, EN83 (2015).
- ³³D. Fall, M. Duquennoy, M. Ouaftouh, N. Smagin, B. Piwakowski, and F. Jenot, *Sens. Actuators A-Phys.* **273**, 303–310 (2018).
- ³⁴M. B. N. Butler, *IEE Proc. F Commun., Radar Signal Process.* **127**, 118 (1980).
- ³⁵G. D. Miller, *Periodically Poled Lithium Niobate: Modeling, Fabrication, and Nonlinear-Optical Performance* (Stanford University, 1998).
- ³⁶R. S. Weis and T. K. Gaylord, *Appl. Phys. A: Solids Surf.* **37**, 191 (1985).
- ³⁷D. Fall, M. Duquennoy, M. Ouaftouh, B. Piwakowski, and F. Jenot, *Ultrasonics* **82**, 371 (2018).
- ³⁸R. M. Ali, St. Ruscheweyh, and E. B. Saff, *Computational Methods and Function Theory 1994—Proceedings Of The Conference* (World Scientific, 1995).
- ³⁹C. C. W. Ruppel, *Advances in Surface Acoustic Wave Technology, Systems and Applications* (World Scientific, 2000).
- ⁴⁰A. A. Tseng, *Nanofabrication: Fundamentals and Applications* (World Scientific, 2008).